DOI: 10.1002/zaac.201100501

Spectral and Structural Studies of Platinum Group Metal Complexes of 3-(Di-2-Pyridylaminomethyl)Benzamide and Formation of Mutual Intermolecular Hydrogen Bonding in Some Complexes

Sairem Gloria,[a] Peng Wang,[b] and Kollipara Mohan Rao*[a]

Keywords: Arene; Pentamethylcyclopentadienyl; Ruthenium; Rhodium; Iridium

Abstract. The new ligand, 3-(di-2-pyridylaminomethyl)benzamide, **L**, which carries two different coordination sites, i.e. the primary amide moiety on one side and a di-2-pyridylamine unit as a strong chelating group on the other side is synthesized. Reaction of chloro-bridged dimers viz., [(η^6-arene)Ru(μ-Cl)Cl]$_2$ and [Cp**M*(μ-Cl)Cl]$_2$ with two equivalents of the ligand **L** in methanol followed by the addition of NH_4BF_4 results the formation of mononuclear complexes of the formulation [(η^6-arene)Ru(**L**)Cl]BF$_4$ [arene = C_6H_6 (**1**), $C_{10}H_{14}$ (**2**), C_6Me_6 (**3**)] and [Cp**M*(**L**)Cl]BF$_4$ [*M* = Rh (**4**); Ir (**5**)]. All these complexes are characterized by micro analyses, IR, and ^{1}H NMR spectroscopic analyses and finally by single crystal XRD study of some representative complexes. Complexes **3** and **5** show mutual intermolecular hydrogen bonding by amide–amide interactions.

1 Introduction

Di-2-pyridylamine-based ligands are employed in different fields of chemistry e. g. metal coordination, supramolecular chemistry,[1–5] as well as the synthesis of new luminescent materials.[6–8] Recently, *Romain* et al. reported the importance of catalytic activity of di-2-pyridylamine ruthenium(II) complexes in the transfer of hydrogenation of aromatic ketones in water.[9] Complexes of Cu^{II},[10] as well as Pd^{II} and Pt^{II}[11,12] with polydipyridylamines were investigated for use in biological applications. Earlier, monomeric complexes bearing di-2-pyridylamine and dimeric complexes with 1,2-bis(di-2-pyridylamino methyl)benzene were reported in our laboratory.[13,14] However, complexes containing a di-2-pyridylamine unit with an amide group at the *meta*-position have not yet been reported. We were interested to synthesize the ligand 3-(di-2-pyridylaminomethyl)benzonitrile and to employ it in the synthesis of heterobimetallic complexes. But because the nitrile group tends to hydrolyze, we ended up in obtaining an amide product. Among the many possible functional groups such as carboxylic acids and alcohols that can be used for the design of hydrogen-bonded networks, amides, in particular primary amides, have been the subject of extensive studies due to the self-complementary nature of its hydrogen-bonded donors/acceptors, but also because of the abundance of amide moieties in biological systems.[15–17] Since simple amides are known to have a free torsion angle about their hydrogen bond it leads to the formation of a range of possible structures with no obvious predictability and certainty.[18]

Herein, we are reporting the synthesis of a new ligand derived from di-2-pyridylamine with an appended benzamide substituent and five new complexes bearing this newly synthesized ligand. For the complexes bearing a symmetrical co-ligand viz., hexamethylbenzene and the pentamethylcyclopentadienyl, a mutual hydrogen bonding network at the amide moiety could be observed, whereas this form of bonding is absent in the *p*-cymene ruthenium complex. The synthesis of the ligand used in this study is shown below (Scheme 1).

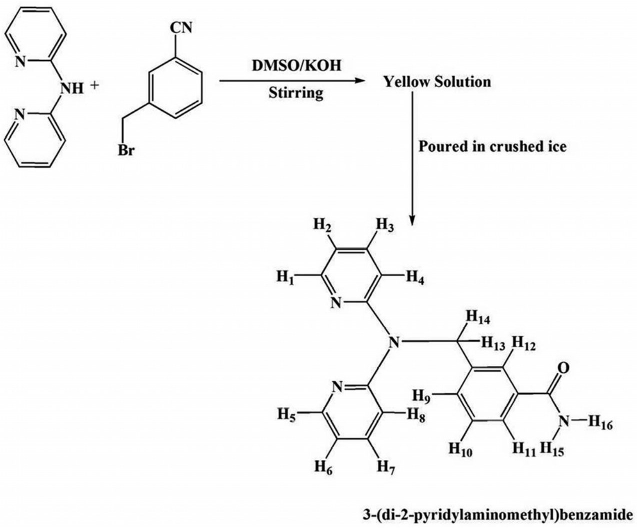

Scheme 1. Schematic diagram for the synthesis of 3-(di-2-pyridylaminomethyl)benzamide.

---

* Prof. Dr. K. M. Rao
Fax: +91-364-2550076
E-Mail: mohanrao59@gmail.com
[a] Department of Chemistry
North Eastern Hill University
Shillong 793 022, India
[b] Department of Chemistry
McMaster University
1280 Main Street West
Hamilton, Ontario L8S 4M1, Canada

2 Results and Discussion

2.1 Ligand Synthesis and Characterization

The ligand 3-(di-2-pyridylaminomethyl)benzamide was synthesized by adopting Steel's procedure.[19] With respect to the starting precursors employed for the preparation of the ligand, we expected to get 3-(di-2-pyridylaminomethyl)benzonitrile; but because of hydrolysis of the nitrile end we obtained the amide product as 3-(di-2-pyridylaminomethyl)benzamide. Since powdered anhydrous sodium hydroxide and potassium hydroxide in DMSO can be used to convert nitriles to amides,[20] this conversion is unambiguous. The conversion of nitrile to amide is confirmed by the disappearance of the nitrile band at around 2236 cm^{-1}, which is present in 3-bromomethylbenzonitrile and the appearance of strong amide I and amide II bands at 1646 and 1593 cm^{-1}, respectively, in the infrared spectrum. The presence of two strong bands at 3390 and 3197 cm^{-1}, respectively, supports the formation of a primary amide and these bands arise from the symmetrical and asymmetrical stretching of the N–H group. The IR spectrum of the ligand also exhibits sharp bands ca. 1474 and 1381 cm^{-1} corresponding to the stretching frequencies of C=C and C=N bonds of the aromatic rings.

The ^1H NMR spectrum of the ligand displays two doublet signals at around 8.31 and 7.16 ppm and two triplet signals at around 7.32 and 6.86 ppm for the pyridyl protons; one singlet signal at δ = 7.82 ppm and a multiplet signal at δ = 7.52 ppm for the phenyl protons; two broad singlet signals for each of the two protons of the $–NH_2$ group at δ = 6.16 and 5.68 ppm and one singlet signal at δ = 5.53 ppm for the $–CH_2–$ protons. The formation of the amide product is also confirmed from the ^{13}C NMR spectrum by the presence of a resonance at 169.4 ppm, which is assigned to the carbonyl carbon of the amide group. Although we were unable to obtain the single crystal XRD structure of the ligand separately, its formation was confirmed by IR, ^1H NMR, and ^{13}C NMR spectroscopic data, and finally from the crystal structures of the complexes.

2.2 [(η^6-arene)Ru(L)Cl]BF_4 [arene = C_6H_6 (1), $C_{10}H_{14}$ (2), C_6Me_6 (3)] and [Cp*M(L)Cl]BF_4 [M = Rh (4), Ir (5)]

Reactions of chloro-bridged dimers, viz. [(η^6-arene)Ru(μ-Cl)Cl]$_2$ and [Cp**M*(μ-Cl)Cl]$_2$ with two equivalents of ligand L in methanol followed by the addition of NH_4BF_4 results the formation of mononuclear complexes of the formulation [(η^6-arene)Ru(L)Cl]BF_4 and [Cp**M*(L)Cl]BF_4, which takes place through chloro-bridge cleavage followed by the dissociation of one chloride ligand of the mentioned starting precursors as shown below (Scheme 2).

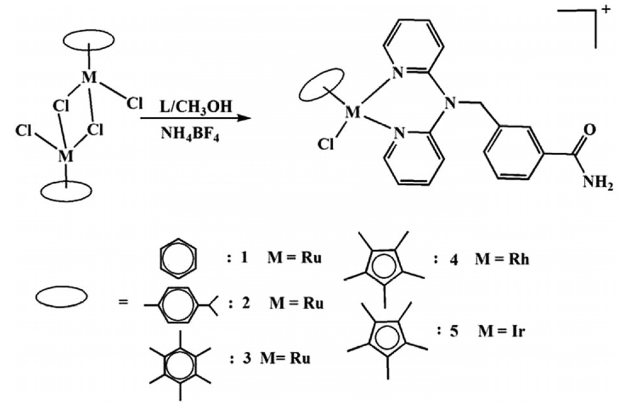

Scheme 2. Syntheses of [(η^6-arene)Ru(L)Cl]BF_4 and [Cp**M*(L)Cl]BF_4 complexes.

These complexes are yellow to orange in color, air stable, non hygroscopic, readily soluble in polar solvents like methanol, dichloromethane, and acetone and sparingly soluble in chloroform but are insoluble in low boiling non-polar solvents like hexane, diethyl ether, and petroleum ether. These complexes are well characterized by micro-analyses, infrared, and ^1H NMR spectral analyses and finally the structures are confirmed from the single crystal XRD analyses of some of the representative complexes and these are discussed below accordingly.

2.2.1 IR Spectroscopic Studies

The IR spectra of the complexes display the symmetric and asymmetric N–H stretching frequency ca.3400 and 3200 cm^{-1}, in which the range remain unaltered when compared with that of the free ligand. This indicates that the amide moiety does not compete strongly with the coordinating site for the binding of central metal atom.[21] This may be due to the fact that the formation of four membered chelate rings around it is not favorable because of steric hindrance. Apart from these bands, the two important bands i.e. the amide I and amide II are also observed at around 1670 and 1600 cm^{-1} resulting from the –C=O and –N–H stretching frequency, respectively. The IR spectra of these complexes also exhibit a sharp bands due to chelated N,N-donor bidentate ligands (ca. 1450 and 1380 cm^{-1}) corresponding to the stretching frequencies of C=C and C=N bonds of the aromatic rings. Since the ligand is neutral, it forms a monocationic complex, in which the charge is balanced by the BF_4 counterion and its ionic nature is thus confirmed from the sharp peak at around 1080 cm^{-1} arising from the $\nu_{B–F}$ stretching frequency.

2.2.2 ^1H NMR Spectroscopic Studies

In the ^1H NMR spectra of complexes **1**–**5**, the signals of the ligands are shifted downfield as compared to those of the free ligand due to the change in electron density after coordination to the central metal atom. The ligand protons of complex **1** resonate in the region 8.97 to 5.52 ppm, whereas for complexes **2** and **3** the protons of the ligand resonate in the region 8.61 to 5.43 ppm and 8.52 to 5.61 ppm, respectively. The details of the assignment of the signals are shown in the Experimental Section. Apart from these ligand signals, complexes **1** and **3** exhibit singlet signals at δ = 6.15 and 1.88 ppm, which represent the proton signals of benzene and the hexamethylbenzene ligand, respectively. The *p*-cymene co-ligand of complex **2** shows two doublet signals at $\delta = 5.63$ and 5.47 ppm for the aromatic protons, a septet signal at $\delta = 2.52$ ppm for the methine proton of the isopropyl group, a singlet signal at $\delta = 2.16$ ppm for the methyl group, and a doublet signal at $\delta = 1.11$ ppm for the methyl protons of the isopropyl group. The ligand protons in complex **4** and **5** resonate in the region 8.73 to 5.80 ppm and 8.70 to 5.57 ppm, respectively. Apart from these ligand signals, complexes **4** and **5** display singlet signals at $\delta = 1.87$ and 2.09 ppm for the pentamethylcyclopentadienyl protons.

The protons of the amide moiety are magnetically and chemically equivalent due to free rotation about the C–N bond and hence display broad singlet signals at $\delta = 5.63$, 5.55, and 5.57 ppm for complexes **1**, **2**, and **5** respectively. For complex **3**, two broad singlet signals are observed at $\delta = 6.97$ and 6.23 ppm due to restricted rotation about the C–N bond. But for complex **4**, the chemical shift value of the amide protons cannot be properly assigned due to overlapping of its broad singlet signal with the doublet signal of the phenyl group at $\delta = 7.43$ ppm.

2.2.3 Molecular Structures and Interactions

In order to confirm the chloride bound cations, crystal structure analyses of some of the representative complexes were carried out, which are discussed below.

The X-ray quality crystals of complex **2** are grown by the slow diffusion of petroleum ether into dichloromethane solution of the complex, which later yielded as yellow block crystals. The crystal is found to crystallize in the monoclinic $P2_1/c$ space group. Molecular structure of complex **2** is shown in Figure 1. The ruthenium cation adopts the expected and usual pseudo-octahedral half sandwich "piano-stool" arrangement around the Ru(1) atom with the *p*-cymene ligand occupying one face of the octahedron and the coordination of the bidentate di-2-pyridylamine moiety and the chloride ion on the other. The Ru(1)–N(31), Ru(1)–N(21) and Ru(1)–Cl bond lengths being 2.107(6), 2.118(7), and 2.418(2) Å, respectively, are within the range of reported arene ruthenium complexes with di-2-pyridylamine.[9,14] The "piano-stool" arrangement about ruthenium atom is further reflected by small bite angle of di-2-pyridylamine moiety N(31)–Ru(1)–N(21) is 84.86(12)°. The metal to arene ring centroid distance is 1.680 Å, which is consistent with the reported value.[9,14]

Due to the presence of this amide moiety, we are expecting a $R^2_2(8)$ and $R^2_4(8)$ motif through hydrogen bonding in this complex. But such types of interactions are not observed; instead, a type of weak interactions involving the amide moiety is observed. The oxygen atom of the carbonyl group acts as an acceptor and is connected to the arene system through one of the aromatic hydrogen atoms of the *p*-cymene co-ligand forming hydrogen bonding (C–H···O) with a bond length of 2.358 Å. Apart from this, one of the hydrogen atoms of the –NH_2 moiety forms a weak interaction with the chlorine atom (N–H···Cl) having the bond length of 2.732 Å, whereas the nitrogen of the same forms a weak interaction with one of the protons of the methyl group of the *p*-cymene co-ligand (C–H···N) with a bond length of 2.731 Å. Consequently, a 1D hydrogen-bonded network is observed as shown in Figure 2, which is entirely different from the expected hydrogen bonding mode.

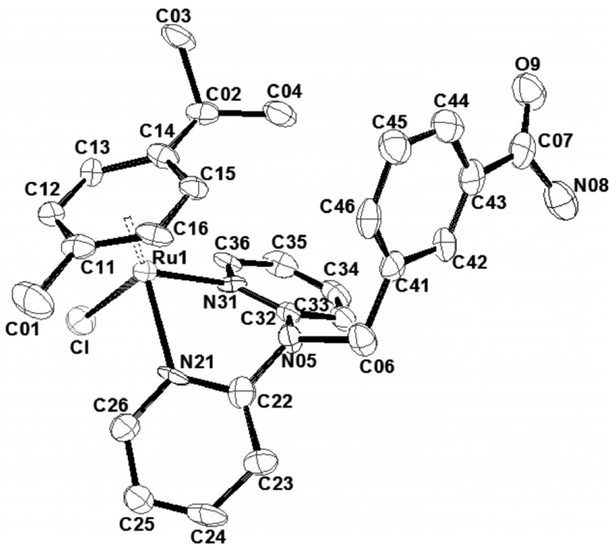

Figure 1. Molecular structure of complex **2** at 45 % probability level. Hydrogen atoms and BF_4^- ions are omitted for clarity. Selected bond lengths /Å and bond angles /°: Ru(1)–Centroid 1.680; Ru(1)–N(21) 2.118(7); Ru(1)–N(31) 2.107(6); Ru(1)–Cl 2.418(2); C(07)–N(08) 1.360(11); C(07)–O(9) 1.197(11); N(31)–Ru(1)–N(21) 84.86(12); N(21)–Ru(1)–Cl 86.7(3); N(31)–Ru(1)–Cl 87.52(18); O(9)–C(07)–N(08) 120.3(11); C(41)–C(06)–N(05) 112.5(8).

Crystals of complex **3** suitable for single crystal XRD analysis are grown and found to crystallize in the triclinic $P\bar{1}$ space group. As in the case of complex **2**, ruthenium cation adopts the "piano-stool" arrangement around the ruthenium atom as shown in Figure 3.

The Ru–N(35), Ru–N(41), and Ru–Cl bond lengths are also in agreement with the reported literatures being in the range 2.0792(18), 2.0842(18), and 2.4068(18) Å, respectively. The metal to arene ring centroid separation is 1.699 Å, whereas the bite angle around N(35)–Ru–N(41) is 80.89(6)°, which are also consistent with the reported value of ruthenium complexes of di-2-pyridylamine.

The single crystal structure of complex **3** shows mutual intermolecular hydrogen bonding network resulting in the formation of 2D sheet like arrangement consisting of various dimeric units. The oxygen atom and one hydrogen atom of the amide moiety of one monomeric unit forms intermolecular hydrogen bonding with nitrogen atom (2.911 Å) and oxygen atom (2.128 Å) of another amide moiety of the other monomeric unit and vice versa adopting an $R^2_2(8)$ like motif. Apart from these one of the hydrogen atoms of the pyridyl moiety of one monomeric unit form weak hydrogen bonding interactions with the oxygen atom and carbon atom of the amide moiety of the neighboring monomeric unit giving rise to a 2D sheet like arrangement as shown in Figure 4.

Single crystals of complex **5** are grown in order to establish the structure of $[Cp^*M(\mathbf{L})Cl]^+$. The representative complex of the formulation $[Cp^*M(L)Cl]^+$ is found to crystallize in the

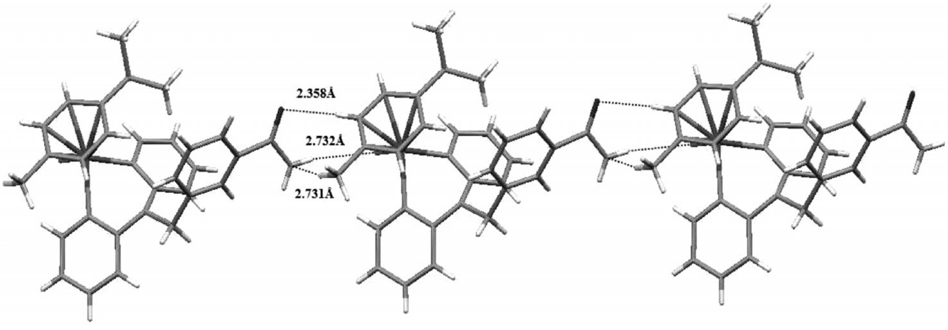

Figure 2. Hydrogen bonding interactions in complex **2** giving rise to a 1D structure.

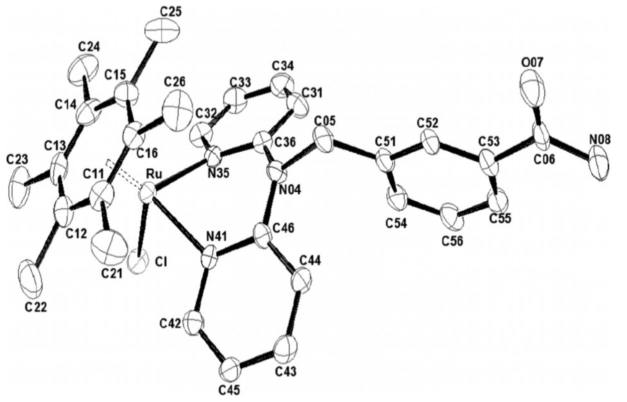

Figure 3. Molecular structure of complex **3** at 45 % probability level. Hydrogen atoms and BF$_4^-$ ionsare omitted for clarity. Selected bond lengths /Å and bond angles /°: Ru(1)–Centroid 1.680; Ru(1)–N(21) 2.118(7); Ru(1)–N(31) 2.107(6); Ru(1)–Cl 2.418(2); C(07)–N(08) 1.360(11); C(07)–O(9) 1.197(11); N(31)–Ru(1)–N(21) 84.86(12); N(21)–Ru(1)–Cl 86.7(3); N(31)–Ru(1)–Cl 87.52(18); O(9)–C(07)–N(08) 120.3(11); C(41)–C(06)–N(05) 112.5(8).

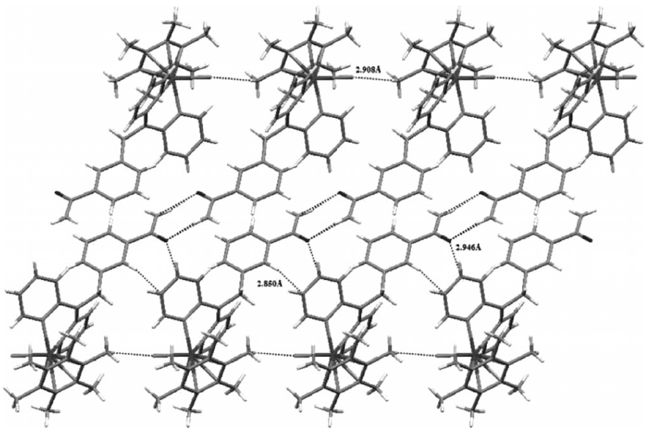

Figure 4. Formation of the 2D sheet like arrangement in complex **3**.

triclinic $P\bar{1}$ space group and is shown in Figure 5. The Ir(1)–N(31), Ir(1)–N(21) and Ir(1)–Cl(1) bond lengths are also in agreement with the reported literatures being in the range 2.087(5), 2.087(5), and 2.397(2) Å, respectively, as reported for the "piano-stool" arrangement complexes of iridium with di-2-pyridylamine. The metal to pentamethylcyclopentadienyl ring centroid separation is 1.783 Å, whereas the bite angle around N(31)–Ir(1)–N(21) is 81.6(2)°. These values are consistent with the reported values.[14]

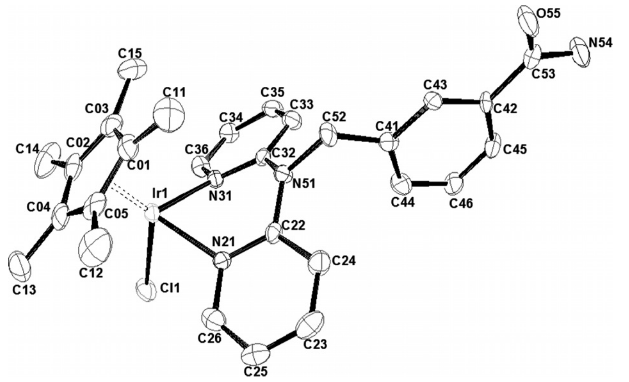

Figure 5. Molecular structure of complex **5** at 45 % probability level. Hydrogen atoms and BF$_4^-$ ions are omitted for clarity. Selected bond lengths /Å and bond angles /°: Ir(1)–Centroid 1.783; Ir(1)–N(21) 2.087(5); Ir(1)–N(31) 2.087(5); Ir(1)–Cl(1) 2.397(2); N(54)–C(53) 1.356(9); O(55)–C(53) 1.236(8); N(31)–Ir(1)–N(21) 81. 6(12); N(21)–Ir(1)–Cl(1) 86.06(17); N(31)–Ir(1)–Cl(1) 87.50(16); O(55)–C(53)–N(54) 120.4(8); N(51)–C(52)–C(41) 116.2(6).

As in the case of complex **3**, the molecular structure of complex **5** shows mutual intermolecular hydrogen bonding resulting in the formation of dimeric unit adopting R$^2_2$(8) motif. The chlorine atom of one monomeric unit exhibits weak interactions with one of the hydrogens of the methyl group of the pentamethylcyclopentadienyl ring and methylene group, respectively. Apart from these interactions, the amide end of the same unit exhibit mutual intermolecular hydrogen bonding with the amide end of another monomeric unit, which already form weak interactions with another monomeric unit through the chlorine atom giving rise to a 2D sheet-like arrangements as shown in Figure 6.

These entire complexes exhibit inter ionic interactions of C–H···F contacts are detected, but these are most probably caused by crystal packing effects and should not affect bond lengths and angles in the molecules.

3 Conclusions

A new di-2-pyridylamine derived ligand, 3-(di-2-pyridylaminomethyl)benzamide, bearing two different interaction sites viz., a primary amide and a di-2-pyridylamine unit cap-

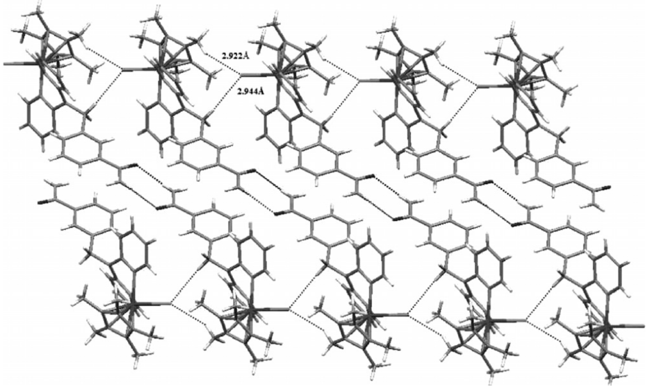

Figure 6. Formation of the 2D sheet like arrangement in complex **5**.

able of forming six membered chelate ring were synthesized. Despite our efforts to prepare dimeric complexes by changing the metal to ligand ratio, changing the solvent and the reaction conditions, only monomeric complexes were obtained. Intermolecular hydrogen bonding resulting in the formation of $R^2_2(8)$ type motif, in which the two monomeric units are connected by a six-membered pseudo ring formed by the amide moieties of each monomer unit are observed in complexes **3** and **5**. This may be attributed to the symmetrical nature of the co-ligand i.e., hexamethylbenzene and pentamethylcyclopentadienyl co-ligand are more symmetrical as compared to the *p*-cymene co-ligand. But the exact reason for exhibiting this type of mutual interaction only in hexamethylbenzene and pentamethylcyclopentadienyl could not be established. Since we are unable to obtain good quality single crystal for complex **1**, we cannot establish the exact mode of bonding in it. But, owing to its similarity with hexamethylbenzene, we would like to conclude that there is possibility of such kind of mutual intermolecular hydrogen bonding mode in it. Although hydrogen-bonded network based on the $R^2_2(8)$ type recognition pattern is observed in complexes **3** and **5**, this does not further connect to form the 2D network $R^2_4(8)$ type motif.

4 Experimental Section

4.1 General Remarks

Infrared spectra were recorded with a Perkin–Elmer Model 983 spectrophotometer with the sample prepared as KBr pellets. The NMR spectra were obtained with a Bruker Avance II 400 spectrometer in $CDCl_3$, [D_3]acetonitrile and [D_6]acetone depending on the solubility of the complexes. Elemental Analyses of the complexes was performed with a Perkin–Elmer 2400 CHN/S analyser. Di-2-pyridylamine and 3-bromomethylbenzonitrile were purchased from Aldrich and used as received. The ligand 3-(di-2-pyridylaminomethyl)benzamide (L) is reported for the first time and the precursor complexes were prepared following the literature procedures.

4.2 X-ray Single Crystal Diffraction and Structure Refinement

X-ray quality crystals from dichloromethane/petroleum ether (complex **2**), dichloromethane/acetone/hexane (complex **3**) and acetone/hexane (complex **5**) were grown as yellow blocks, orange bars, and yellow plates, respectively. The intensity data for the complexes were collected with a STOE IPDS II diffractometer with Mo-K_α radiation in the whole reciprocal sphere. A numerical absorption correction was based on the crystal shape that was originally derived from the optical face indexing but was later optimized against equivalent reflections using the STOE X-shape software.[22] Structures were refined with full-matrix least-squares on F^2 using SHELXL-97.[23] All non-hydrogen atoms were refined anisotropically. The hydrogen atoms were located from the difference Fourier maps and refined. Structural illustrations were drawn with ORTEP-3[24] for Windows. The ORTEP presentations of the representative complexes are shown in Figure 1, Figure 3, and Figure 5. Crystallographic data collection parameters are presented in Table 1.

Crystallographic data (excluding structure factors) for the structures in this paper have been deposited with the Cambridge Crystallographic Data Centre, CCDC, 12 Union Road, Cambridge CB21EZ, UK. Copies of the data can be obtained free of charge on quoting the depository numbers CCDC-853730 (**2**), CCDC-853731 (**3**), and CCDC-853732 (**5**) (Fax: +44-1223-336-033; E-Mail: deposit@ccdc.cam.ac.uk, http://www.ccdc.cam.ac.uk),

4.3 Synthesis of the Ligand

Di-2-pyridylamine (0.314 g, 1.83 mmol) and potassium hydroxide (0.377 g, 6.73 mmol) were given in a round-bottomed flask (50 mL). To the mixture, DMSO (25 mL) was added and left stirring until the potassium hydroxide flakes dissolved and a clear yellow solution was obtained. Afterwards, 3-bromomethylbenzonitrile (0.300 g, 1.53 mmol) was added and further stirred for overnight to ensure that the reaction was complete. The clear yellow solution was poured into crushed ice (200 g) and left to stand for some time during which a pale yellow precipitate was obtained. The precipitate was filtered, dried, and recrystallized from methanol to yield the pale yellow microcrystalline product. Yield: 0.270 g (58 %); Melting Point: 80 °C; Elemental Anal. $C_{18}H_{16}N_4O$: calcd. C 71.04; H 5.30; N 18.41 %; found C 70.95; H 5.22; N 18.16 %. **IR** (KBr): $\tilde{\nu}$ = 3390 ($\nu_{N–H\ (asymmetric)}$); 3197 ($\nu_{N–H\ (symmetric)}$); 1646 ($\nu_{C=O}$, amide I); 1593 ($\nu_{N–H}$, amide II); 1474–1381 ($\nu_{C=C}$, $\nu_{C=N\ (aromatic)}$) cm^{-1}. **^{1}H NMR** ($CDCl_3$, 400 MHz, 25 °C): δ = 8.31 (d, J = 3.6 Hz, 2 H, H_1 and H_5); 7.82 (s, 1 H, H_{12}); 7.63 (d, J = 7.6 Hz, 2 H, H_4 and H_8); 7.52 (m, J = 8.4 Hz, 1.2 Hz, 2 H, H_{10} and H_{11}); 7.32 (t, J = 7.6 Hz, 2 H, H_2 and H_6); 7.16 (d, J = 8.4 Hz, 1 H, H_9); 6.86 (t, J = 6.8 Hz, 2 H, H_3 and H_7); 6.16 (s (broad), 1 H, H_{15}); 5.68 (s (broad), 1 H, H_{16}); 5.53 (s, 2 H, H_{13} and H_{14}) ppm. **^{13}C{^{1}H} NMR** ($CDCl_3$, 100 MHz, 25 °C): δ = 169.4 (1C, C=O); 156.1 (2C, dipyridyl); 147.5 (2C, dipyridyl); 138.9 (1C, phenyl); 138.2 (2C, dipyridyl); 130.816 (1C, phenyl); 128.7 (1C, phenyl); 126.5 (1C, phenyl); 126.3 (2C, phenyl); 117.7 (2C, dipyridyl); 114.9 (2C, dipyridyl); 51.5 (1C, $–CH_2–$) ppm.

*4.4 General Procedure for the Preparation of [(η^6-arene)Ru(L)Cl]BF_4 [arene = C_6H_6 (1), $C_{10}H_{14}$ (2), C_6Me_6 (3)] and [Cp*M(L)Cl]BF_4 [M = Rh (4), Ir (5)]*

A mixture of 3-(di-2-pyridylaminomethyl)benzamide (0.050 g, 0.164 mmol) and [(η^6-arene)Ru(μ-Cl)Cl]$_2$ (0.082 mmol) for complexes **1**–**3** or [Cp*M(μ-Cl)Cl]$_2$ (0.082 mmol) for complexes **4** and **5** were stirred in methanol (25 mL) until a clear yellow solution was obtained. Afterwards, two equivalents of NH_4BF_4 were added and continued to stir for another 10 h to ensure that the reaction was complete. The yellow solution was evaporated under reduced pressure to yield

Table 1. Crystal data and structure refinement for complexes **2**, **3**, and **5**.

	2	**3**	**5**
Chemical formula	$C_{28}H_{30}BClF_4N_4ORu$	$C_{30}H_{34}BClF_4N_4ORu$	$C_{28}H_{31}BClF_4IrN_4O$
Formula weight	661.89	689.94	754.05
Crystal system	monoclinic	triclinic	triclinic
Space group	$P2_1/c$	$P\bar{1}$	$P\bar{1}$
Crystal color and shape	yellow block	orange bar	yellow plate
Crystal size /mm^3	0.21 × 0.18 × 0.15	0.26 × 0.14 × 0.12	0.31 × 0.24 × 0.14
a /Å	12.757(3)	8.2081(16)	7.9714(16)
b /Å	17.307(4)	12.550(3)	12.399(3)
c /Å	14.346(3)	15.356(6)	15.688(3)
α /°	90.00	66.56(2)	111.33(3)
β /°	115.32(3)	85.28(4)	93.12(3)
γ /°	90.00	84.63(3)	91.32(3)
V /Å^3	2862.9(10)	1443.2(7)	1440.7(5)
Z	4	2	2
T /K	293(2)	293(2)	293(2)
D_c /g·cm^{-3}	1.536	1.588	1.738
μ /mm^{-1}	0.696	0.694	4.802
θ range for data collection /°	1.77 to 29.28.	1.45 to 26.62	1.77 to 29.14
Unique reflections	22519	17041	20515
R_{int}	0.2048	0.1521	0.1042
Final R indices [$I > 2\sigma(I)$]$^{a)}$	$R_1 = 0.0599$, $wR_2 = 0.0650$	$R_1 = 0.0569$, $wR_2 = 0.0849$	$R_1 = 0.0434$, $wR_2 = 0.0524$
R indices (all data)	$R_1 = 0.2710$, $wR_2 = 0.0988$	$R_1 = 0.1187$, $wR_2 = 0.0988$	$R_1 = 0.1334$, $wR_2 = 0.0654$
Goodness-of-fit	0.657	0.830	0.623
Max, min $\Delta\rho$ /e·Å^{-3}	0.696, –0.570	0.658, –0.683	1.159, –1.155

a) Structures were refined on F_o^2: $wR_2 = [\Sigma[w(F_o^2–F_c^2)^2]/\Sigma w(F_o^2)^2]^{1/2}$, where $w^{-1} = [\Sigma(F_o^2)+(aP)^2+bP]$ and $P = [\max(F_o^2, 0)+2F_c^2]/3$.

the yellow residue, which was extracted with dichloromethane. The dichloromethane solution of the complex was finally layered with diethyl ether and left for one day to yield the yellow microcrystalline complexes.

Complex 1: Yield 0.061 g (50 %); Elemental Anal. $C_{24}H_{22}BClF_4N_4ORu$: calcd. C 47.54; H 3.66; N 9.24 %; found C 47.03; H 3.52; N 9.03 %. **IR** (KBr): $\tilde{\nu}$ = 3429 ($\nu_{N–H\ (asymmetric)}$) 3184 ($\nu_{N–H\ (symmetric)}$); 1659 ($\nu_{C=O}$, amide I); 1600 ($\nu_{N–H}$, amide II); 1447–1407 ($\nu_{C=C}$, $\nu_{C=N\ (aromatic)}$); 1076 ($\nu_{B–F}$) cm^{-1}. **^{1}H NMR** ([D$_6$]acetone, 400 MHz, 25 °C): δ = 8.97 (d, J = 4.8 Hz, 2 H, H$_1$ and H$_5$); 8.11 (s, 1 H, H$_{12}$); 8.02 (t, J = 7.6 Hz, 2 H, H$_2$ and H$_6$); 7.91 (d, J = 7.6 Hz, 2 H, H$_3$ and H$_7$); 7.85 (d, J = 7.6 Hz, 1 H, H$_9$); 7.62 (d, J = 8.4 Hz, 1 H, H$_{11}$); 7.55 (t, J = 7.6 Hz, 2 H, H$_3$ and H$_7$); 7.30 (t, J = 6.4 Hz, 1 H, H$_{10}$); 6.15 (s, 6 H, C_6H_6); 5.63 (s, 2 H, H$_{15}$ and H$_{16}$); 5.52 (s, 2 H, H$_{13}$ and H$_{14}$) ppm.

Complex 2: Yield 0.075 g (69 %); Elemental Anal. $C_{28}H_{30}BClF_4N_4ORu$: calcd. C 50.80; H 4.56; N 8.46 %; found C 50.67; H 4.31; N 8.34 %. **IR** (KBr): $\tilde{\nu}$ = 3416 ($\nu_{N–H\ (asymmetric)}$); 3197 ($\nu_{N–H\ (symmetric)}$); 1666 ($\nu_{C=O}$, amide I); 1600 ($\nu_{N–H}$, amide II); 1460–1387 ($\nu_{C=C}$, $\nu_{C=N\ (aromatic)}$); 1082 ($\nu_{B–F}$) cm^{-1}. **^{1}H NMR** (CDCl$_3$, 400 MHz, 25 °C): δ = 8.61 (d, J = 5.2 Hz, 2 H, H$_1$ and H$_5$); 8.02 (s, 1 H, H$_{12}$); 7.87 (d, J = 7.6 Hz, 2 H, H$_4$ and H$_8$); 7.79 (t, J = 7.2 Hz, 2 H, H$_2$ and H$_6$); 7.44 (d, J = 5.6 Hz, 1 H, H$_9$); 7.38 (t, J = 7.6 Hz, 2 H, H$_3$ and H$_7$); 7.31 (d, J = 8.0 Hz, 1 H, H$_{11}$); 7.13 (t, J = 6.8 Hz, 1 H, H$_{10}$); 5.63 (d, J = 4.8 Hz, 2 H, aromatic-cymene); 5.55 (s, 2 H, H$_{15}$ and H$_{16}$); 5.47 (d, J = 5.2 Hz, 2 H, aromatic- cymene); 5.43 (s, 2 H, H$_{13}$ and H$_{14}$); 2.52 [sept, 1 H, J = 6.8 Hz C*H*(CH$_3$)$_2$]; 2.16 (s, 3 H, -CH$_3$); 1.11 [d, J = 6.8 Hz, 6 H, CH(C*H*$_3$)$_2$] ppm.

Complex 3: Yield 0.072 g (70 %); Elemental Anal. $C_{30}H_{34}BClF_4N_4ORu$: calcd. C 52.21; H 4.96; N 8.12 %; found C 52.08; H 4.94; N 8.07 %. **IR** (KBr): $\tilde{\nu}$ = 3403 ($\nu_{N–H\ (asymmetric)}$); 3191 ($\nu_{N–H\ (symmetric)}$); 1672 ($\nu_{C=O}$, amide I); 1600 ($\nu_{N–H}$, amide II); 1447–1381 ($\nu_{C=C}$, $\nu_{C=N\ (aromatic)}$); 1082 ($\nu_{B–F}$) cm^{-1}. **^{1}H NMR** ([D$_3$]acetonitrile, 400 MHz, 25 °C): δ = 8.52 (dd, J = 5.6 Hz, 2 H, H$_1$ and H$_5$); 7.90 (d, J = 7.6 Hz, 2 H, H$_4$ and H$_8$); 7.85 (t, J = 8.0 Hz, 1 H, H$_{10}$); 7.74 (s, 1 H, H$_{12}$); 7.52 (t, J = 6.8 Hz, 2 H, H$_2$ and H$_6$); 7.46 (d, J = 8.0 Hz, 1 H, H$_9$); 7.32 (t, J = 6.8 Hz, 2 H, H$_3$ and H$_7$); 7.19 (d, J = 8.4 Hz, 1 H, H$_{11}$); 6.97 [s (broad), 1 H, H$_{15}$]; 6.23 [s (broad), 1 H, H$_{16}$]; 5.61 (s, 2 H, H$_{13}$ and H$_{14}$); 1.88 (s, 18 H, C_6Me_6) ppm.

Complex 4: Yield 0.075 g (70 %); Elemental Anal. $C_{28}H_{31}BClF_4N_4ORh$: calcd. C 50.59; H 4.70; N 8.42 %; found C 50.25; H 3.99; N 8.36 %. **IR** (KBr): $\tilde{\nu}$ = 3449 ($\nu_{N–H\ (asymmetric)}$); 3191 ($\nu_{N–H\ (symmetric)}$); 1672 ($\nu_{C=O}$, amide I); 1600 ($\nu_{N–H}$, amide II); 1447–1381 ($\nu_{C=C}$, $\nu_{C=N\ (aromatic)}$); 1076 ($\nu_{B–F}$) cm^{-1}. **^{1}H NMR** ([D$_6$]acetone), 400 MHz, 25 °C): δ = 8.73 (d, J = 6.0 Hz, 2 H, H$_1$ and H$_5$); 8.08 (t, J = 8.8 Hz, 2 H, H$_2$ and H$_6$); 8.01 (d, J = 6.4 Hz, 2 H, H$_4$ and H$_8$); 7.66 (d, J = 8.0 Hz, 1 H, H$_9$); 7.58 (t, J = 8.0 Hz, 2 H, H$_3$ and H$_7$); 7.50 (t, J = 6.4 Hz, 1 H, H$_{10}$); 7.43 (d, J = 8.8 Hz, 1 H, H$_{11}$); 6.63 (s, 1 H, H$_{12}$); 5.80 (s, 2 H, H$_{13}$ and H$_{14}$); 1.87 (s, 15 H, Cp*) ppm.

Complex 5: Yield 0.064 g (67 %); Elemental Anal. $C_{28}H_{31}BClF_4N_4OIr$: calcd. C 44.60; H 4.14; N 7.43 %; found C 44.52; H 4.12; N 7.26 %. **IR** (KBr): $\tilde{\nu}$ = 3403 ($\nu_{N–H\ (asymmetric)}$); 3191 ($\nu_{N–H\ (symmetric)}$); 1666 ($\nu_{C=O}$, amide I); 1600 ($\nu_{N–H}$, amide II); 1460–1381 ($\nu_{C=C}$, $\nu_{C=N\ (aromatic)}$); 1076 ($\nu_{B–F}$) cm^{-1}. **^{1}H NMR** ([D$_6$]acetone, 400 MHz, 25 °C): δ = 8.77 (dd, J = 1.6 Hz, 4.4 Hz, 2 H, H$_1$ and H$_5$); 8.06–7.98 (m, J = 1.6 Hz, 7.2 Hz, 3 H, H$_9$, H$_{10}$ and H$_{11}$); 7.67 (d, J = 7.6 Hz, 2 H, H$_4$ and H$_8$); 7.60 (t, J = 2.0 Hz, 2 H, H$_2$ and H$_6$); 7.47 (s, 1 H, H$_{12}$); 7.43 (t, J = 4.8 Hz, 2 H, H$_3$ and H$_7$); 5.76 (s, 2 H, H$_{13}$ and H$_{14}$); 5.57 (s, 2 H, H$_{15}$ and H$_{16}$); 2.09 (s, 15 H, Cp*) ppm.

Acknowledgement

Sairem Gloria thanks *UGC*, New Delhi for providing financial assistance in the form of University Fellowship. K. M. Rao gratefully acknowledges financial support from the *UGC*, New Delhi, through the Research grant No. F.No.39–793/2010 (SR).

References

[1] S. Demeshko, G. Leibeling, S. Dechert, F. Meyer, *Dalton Trans.* **2004**, 3782–3787.

[2] C. Seward, W. l. Jia, R. Y. Wang, S. Wang, *Inorg. Chem.* **2004**, *43*, 978–985.

[3] P. Gamez, P. de Hoog, O. Roubeau, M. Lutz, W. L. Driessen, A. L. Spek, J. Reedijk, *Chem. Commun.* **2002**, 1488–1489.

[4] P. de Hoog, P. Gamez, M. Leuken, O. Roubeau, B. Krebs, J. Reedijk, *Inorg. Chim. Acta* **2004**, *357*, 213–218.

[5] W. L. Jia, D. R. Bai, T. McCormick, Q. D. Liu, M. Motala, R. Y. Wang, C. Seward, Y. Tao, S. Wang, *Chem. Eur. J.* **2004**, *10*, 994–1006.

[6] Q. D. Liu, W. L. Jia, G. Wu, S. Wang, *Organometallics* **2003**, *22*, 3781–3791.

[7] Y. Kang, C. Seward, D. Song, S. Wang, *Inorg. Chem.* **2003**, *42*, 2789–2797.

[8] C. Seward, W. L. Jia, R. Y. Wang, G. D. Enright, S. Wang, *Angew. Chem. Int. Ed.* **2004**, *43*, 2933–2936.

[9] C. Romain, S. Gaillard, M. K. Elmkaddem, L. Toupet, C. Fischmeister, C. M. Thomas, J.-L. Renaud, *Organometallics* **2010**, *29*, 1992–1995.

[10] T. Chao, Y. Shao, N. Gan, Q. Xu, Z. Guo, *Inorg. Chem.* **2004**, *43*, 4761–4766.

[11] C. Tu, J. Lin, Y. Shao, Z. Guo, *Inorg. Chem.* **2003**, *42*, 5795–5797.

[12] S. Fakih, W. C. Tung, D. Eierhoff, C. Mock, B. Krebs, *Z. Anorg. Allg. Chem.* **2005**, *631*, 1397–1402.

[13] G. Gupta, S. Gloria, B. Das, K. M. Rao, *J. Mol. Struct.* **2010**, *979*, 205–213.

[14] G. Gupta, S. Gloria, B. Therrien, B. Das, K. M. Rao, *J. Organomet. Chem.* **2011**, *696*, 702–708.

[15] J. C. MacDonald, G. M. Whitesides, *Chem. Rev.* **1994**, *71*, 2383–2420.

[16] G. R. Desiraju, *Angew. Chem. Int. Ed. Engl.* **1995**, *34*, 2311–2327.

[17] C. B. Aakeröy, B. M. T. Scott, J. Desper, *New J. Chem.* **2007**, *31*, 2044–2051.

[18] J. J. Kane, T. Nguyen, J. Xiao, F. W. Fowler, J. W. Lauher, *Mol. Cryst. Liq. Cryst.* **2001**, *356*, 449–458.

[19] B. Antonioli, D. J. Bray, J. K. Clegg, K. Gloe, K. Gloe, O. Kataeva, L. F. Lindoy, J. C. McMurtrie, P. J. Steel, C. J. Sumby, M. Wenzel, *Dalton Trans.* **2006**, 4783–4794.

[20] W. Roberts, M. C. Whiting, *J. Chem. Soc.* **1965**, 1290–1293.

[21] S. A. Baudron, D. S. Mendoza, M. W. Hosseini, *CrystEngComm* **2009**, 1245–1254.

[22] Stoe & Cie *X-SHAPE*, Version 2.05: Program for Crystal Optimization for Numerical Absorption Correction; Stoe & Cie GmbH, Darmatadt, Germany, **2004**.

[23] G. M. Sheldrick, *SHELXL-97*, Program for Crystal Structure Refinement, University of Göttingen, Göttingen, Germany, **1997**.

[24] L. J. Farrugia, *J. Appl. Crystallogr.* **1997**, *30*, 565–566.

Received: November 16, 2011